EE12-2 More Sustainable Masonry Façades: Preheating Ventilation Air Using a Dynamic Buffer Zone (DBZ)[1]

R.C. Richman[2], C. Cianfrone,[3] and K.D. Pressnail[4]

Abstract

During sunny conditions, surface temperatures on masonry façades can rise to over 40 degrees centigrade above the ambient temperatures. Conventional wall designs minimize the benefits of this solar heat through the use of thermal insulation. However, air that is drawn from the outdoors, between the façade and sheathing, can be used to recover heat from the masonry. The system, which utilizes a Dynamic Buffer Zone (DBZ), acts as a solar air collector. This system can provide an effective way to preheat ventilation air at little to no extra cost while not compromising the architectural features of the masonry wall system. A numerical model was developed to predict the amount of heat recovery possible using a DBZ. The numerical model was verified by comparing results with a commercial computational fluid dynamics software package and by conducting laboratory experiments. Preliminary results indicate that the DBZ as a solar air collector can achieve as high as 33% daily solar efficiency and seasonal solar efficiencies of up to 27%. Since this system is low-cost, yet effective, it may offer designers an opportunity to build more sustainable masonry wall systems.

Keywords: ventilated façades, masonry, energy efficiency, sustainability, dynamic buffer zone, energy conservation

Introduction

Conventional methods and fuels for providing energy are becoming increasingly expensive and their by-products are contributing to global warming and climate change. In order to minimize the overall impact of the human species, there needs to exist an urgent and aggressive energy strategy that addresses conservation, energy efficiency and renewable power. In Canada, buildings account for over 30% of the total energy consumed [1]. Given that over 50% of this is for space heating, a large potential exists for energy savings [1]. Some current solutions for energy savings include small-scale renewable power, conservation by homeowners, and innovative designs that

---

[1] This conference input is based on paper accepted to Journal of Building Physics and published with permission of the Sage Corporation

[2] Assistant Professor, Dept of Architectural Science, Ryerson U, Toronto, ON, M5B 2K3, , richman@ryerson.ca

[3] M.A.Sc., P. Eng., , Morrison Hershfield Ltd., Toronto, ON, M2J 1T1, Canada, ccianfrone@morrisonhershfield.com

[4] Associate Professor, Dept of Civil Engineering, Uf Toronto, Toronto, ON, M5S 1A4, pressna@ecf.utoronto.ca

encourage energy efficiency and use on-site renewable resources. [2, 3] This article summarizes research of a ventilated masonry façade used for preheating ventilation air.

Ventilated façades as a method of controlling solar energy is not a new idea. The most common application is the Trombe wall, originally patented in 1881 by Edward Morse [4], but not popularized until Felix Trombe [5] patented a similar system in 1972. Since 1972, significant research has been conducted on similar systems and approaches [6-10]. Ventilated façades that do not include glazing have been studied much less than those with glazing such as the Trombe wall. The work in unglazed ventilated façade systems is limited and mainly focuses on the ability of ventilated façades to reduce summer cooling loads in buildings [11, 12]. To date, most of the work in this area includes numerical analysis to describe the behaviour and energy performance of ventilated façades, however literature on experimental data is scarce. The need for research focussing on ventilated facades as useful tools in cold climates during the heating season is evident [13-15]. This research also extends on ideas founded by research on recovering heat through dynamic insulation [16-18]

Work has been completed in the area of dynamic buffer zones (DBZ), an active ventilated façade type characterized by a buffer zone (i.e. usually a cavity in the wall) pressurized to control the migration of bulk moisture through air leakage [19, 20]. Further investigation suggested the possibility of using a DBZ as a method of thermal control [21]. Recent research documents a Solar DBZ (DBZ) used as an effective means of preheating ventilation air through curtain walls [15].

This paper presents research of a DBZ within a masonry façade used to reduce space heating loads in cold climates. Using computer simulation and laboratory scale model testing, this research shows the DBZ to be a simple, more sustainable, energy efficient and low-cost approach to traditional wall assemblies.

The DBZ Applied to a Masonry Façade Wall Assembly

The physical aspect of the DBZ wall was modeled after typical construction methods. Focus was placed on residential applications, which is reflected in the design and experimental as shown in Figure 1. The construction of the wall, from outside to inside, is (further detail can be found in [22]:

- 90mm brick, variable depth air cavity
- 50mm extruded polystyrene insulation
- 39mm x 89mm wood stud cavity
- 400mm apart and filled with fibreglass batt insulation

- polyethylene vapour retarder
- 12.5mm gypsum board

There are many factors that contribute to the amount of heat being transferred between the various parts of the DBZ system. These include incoming solar radiation, ambient conditions, air cavity velocity, and cavity dimensions. Solar radiation and ambient conditions are not under the designer's control, however thickness of the airspace and cavity velocity are variables that were considered in the design process. Since the DBZ is a tool for preheating ventilation air, the overall flow through the cavity is fixed according to the ventilation requirements of the interior space. However, the cavity velocity via the air space thickness, can be varied for optimal performance.

Numerical and experimental analysis in this research considered a single wall type, that of a typical residential wall in southeastern Ontario, Canada:

- 89mm brick
- 25mm unvented air space
- 38mm extruded polystyrene insulation
- 39 x 89 mm studs filled with 89mm fibreglass batt insulation
- polyethylene vapour retarder
- 12.5mm gypsum board.

The DBZ wall uses the same construction, with the exception of the unvented air space. The DBZ airspace is of a thickness that optimizes performance, and it is a vented cavity, drawing air at the bottom of the wall from the outdoors, and delivering it to the interior at the top of the wall, as shown in Figure 1.

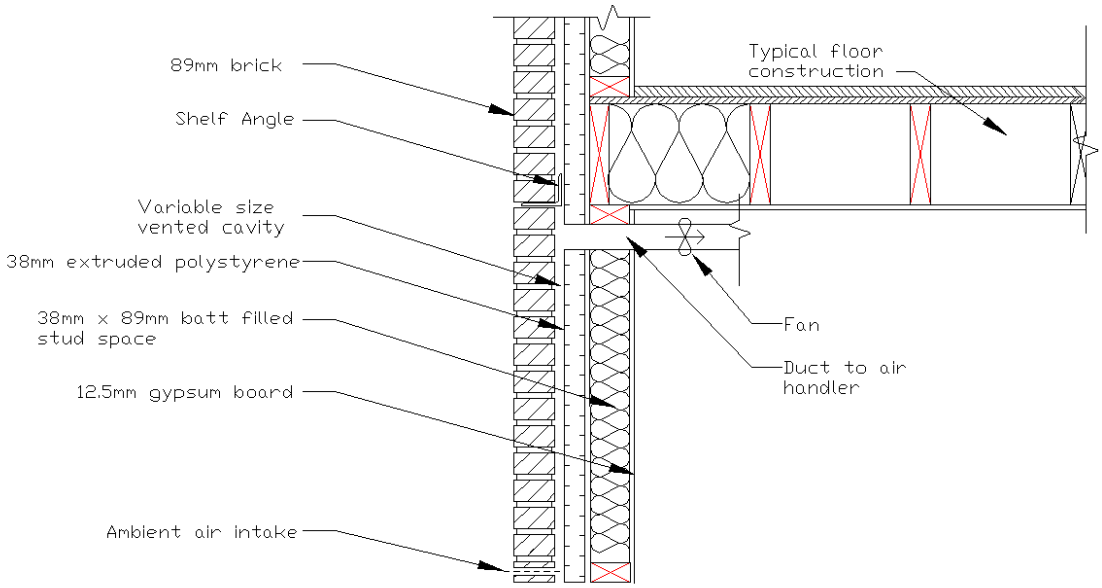

Figure 1 – Cross-sectional View of Conceptual Design

Numerical Model

Several heat transfer mechanisms take place in the DBZ wall and can be accounted for mathematically by defining a heat balance equation for each surface of the wall in addition to one for the air that enters and exits the wall. Figure 2 graphically shows the one-dimensional numerical model developed in this work. Equations 1 through 5 present the numerical model.

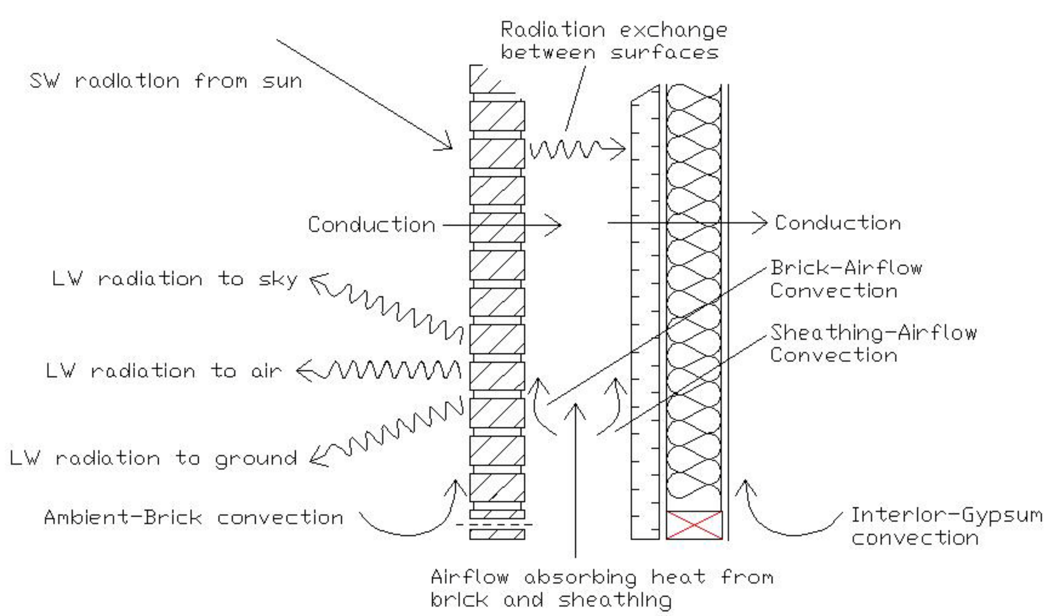

Figure 2 – Heat Transfer Mechanisms for a DBZ Wall

The equations are defined per surface (4 equations), and one for air. The exterior insulation, stud cavity and gypsum board is defined as one assembly for the numerical model, where one surface is the outer exterior insulation and the other is the interior gypsum board. The assumptions for the heat balance equations are:

1. The brick is the only component that experiences thermal storage (modeled on the exterior surface of the brick.)
2. One-dimensional heat flow to the sides is negligible and heat flux is unidirectional, i.e. perpendicular to air flow.
3. The inlet air temperature is equal to the exterior air temperature.
4. The exterior ground temperature is equal to the ambient air temperature [23].
5. The surface temperature does not change with height.
6. A weighted mean fluid temperature as provided by Eicker [24] is a good approximation in lieu of integrating over the entire height of the surface.
7. The sky temperature is approximated by the Bliss correlation [25].

In the equations 1 through 5, the convention used assumes that heat flux into the surface is on the left and heat flux out of the surface is on the right of each equation. The equations describe the exterior brick surface, interior brick surface, cavity air, exterior insulation surface, and interior gypsum board surface, respectively.

Exterior Brick Surface

$$\begin{aligned}\alpha E_t A &= h_{eb} A (T_{eb} - T_a) + h_{r,grd} A (T_{eb} - T_{grd}) + h_{r,sky} A (T_{eb} - T_{sky}) + h_{r,air} A (T_{eb} - T_a) \\ &+ U_b A (T_{eb} - T_{ib}) + \rho_b c_{p,b} V_b \left(\frac{dT_{eb}}{dt} \right)\end{aligned} \tag{1}$$

Interior Brick Surface

$$U_b A (T_{eb} - T_{ib}) = h_{ib} A (T_{ib} - T_{f,m}) + h_{r,cav} A (T_{ib} - T_{ins}) \tag{2}$$

Cavity Air

$$\dot{m} c_{p,a} (T_{ea} - T_{ia}) = h_{ib} A (T_{ib} - T_{f,m}) + h_{ins} A (T_{ins} - T_{f,m}) \tag{3}$$

Exterior Insulation Surface

$$h_{r,cav} A (T_{ib} - T_{ins}) = U_{ins} A (T_{ins} - T_{gyp}) + h_{ins} A (T_{ins} - T_{f,m}) \tag{4}$$

Interior Gypsum Board Surface

$$U_{ins} A\left(T_{ins} - T_{gyp}\right) = h_i A\left(T_{gyp} - T_i\right) \tag{5}$$

For the heat transfer coefficient between the interior gypsum board surface and the interior room air and surroundings, a combined heat transfer coefficient was used ($h_i = 8.29$, [24]).

The convection coefficient was derived from the correlation provided by[25]. The correlation is for two parallel plates with constant heat flux on one side and insulated on the other.

$$Nu = 5.4 + \frac{0.00190\left(\mathrm{Re}\,\mathrm{Pr}\, d_h / L\right)^{1.71}}{1 + 0.00563\left(\mathrm{Re}\,\mathrm{Pr}\, d_h / L\right)^{1.17}}$$

Verification of the Numerical Model

The numerical model mathematically describes the DBZ system and provides an effective tool in estimating energy reductions from the system under various scenarios. In order to test the accuracy of this model, it was solved under varying conditions and the results were compared with scale model experimental results .

A test wall, shown in Figure 3, was built between simulated interior and exterior (sunny winter day) climates. Exterior air was introduced at the bottom of the test wall on the winter side at different flow rates. Heat lamps simulating solar radiation were placed on the cold side of the wall and the incoming air was collected through a manifold at the top of the wall on the warm side. The increase in air temperature was investigated as well as each of the surface temperatures in the wall assembly. The test wall section was constructed exactly as shown in Figure 1, with the following notable features:

- The height of the test wall was 1.8 m and the width spanned three wood framing members, each 0.4 m apart.
- The inlet vents extend the entire width of the test wall along the bottom and are 0.08 mm high. This setup was chosen to allow for the most uniform inlet flow.
- The outlet manifold extends the entire width of the wall at the top of the cavity, collecting air in the vertical direction and then changing to the horizontal direction. The manifold gradually changes shape from rectangular to round.
- A variable speed blower is attached to the end of the manifold and draws in exterior air up the cavity, through the manifold, and out the other side of the blower.

- The test wall was constructed to be air tight and highly insulated around the perimeter to minimize heat loss at the edges.
- Four thermocouples were distributed evenly on each surface and averaged out to obtain one average value per surface. An additional three thermocouples were installed in both the inlet and exit air streams.
- The air velocity was taken at several locations using a Mini-Vane Thermo-Anemometer. Measurements were taken at the bottom of the wall, where the cold air enters the cavity.
- 10 x 250W clear Philips Heat Lamps (250BR40) were installed on a rack with five rows and two columns, evenly distributed along the height and width of the test area.

Figure 3 – Photograph of the Test Wall During Experimental Testing

Steady state experimental data was taken at three flow rates – 21, 36, and 72.5 $m^3/h/m^2$ – the results then compared to the numerical model with similar boundary conditions. Figures 4, 5 and 6 show this graphically.

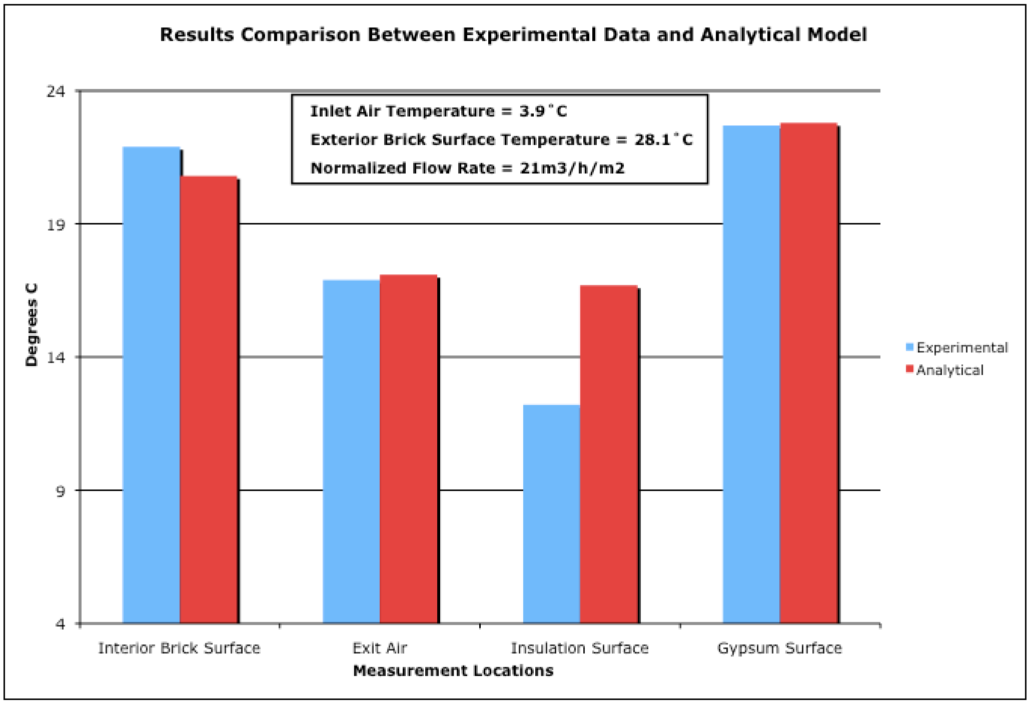

Figure 4 – Comparison of surface and air temperatures experiments and numerical model ($21m^3/h/m^2$ normalized flow rate)

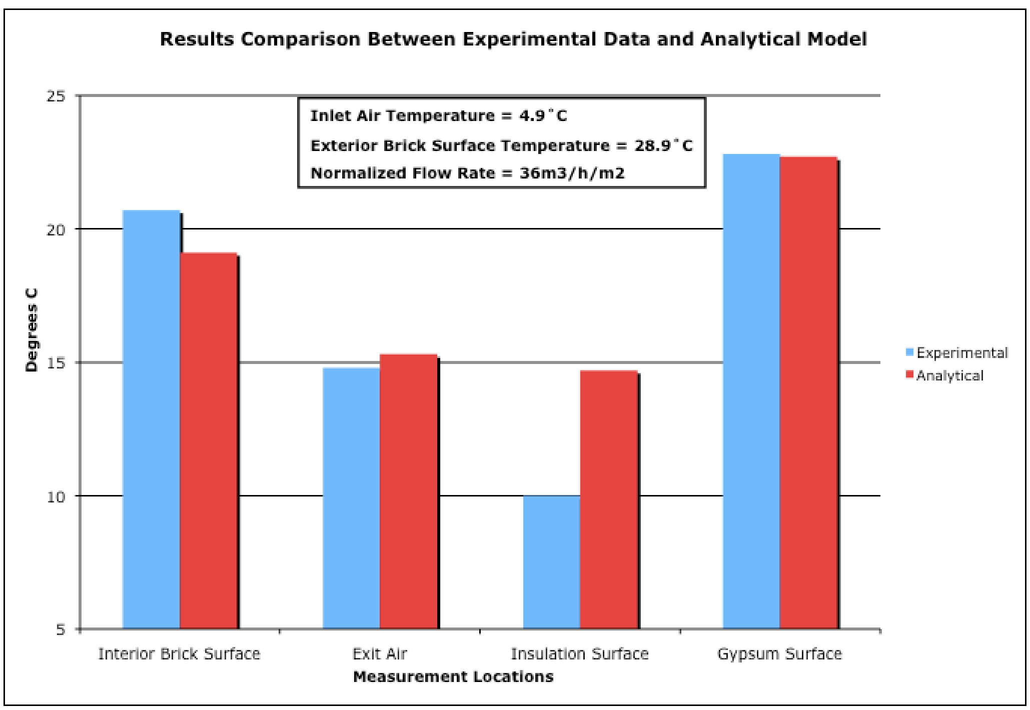

Figure 5 – Comparison of surface and air temperatures experiments and numerical model ($36m^3/h/m^2$ normalized flow rate)

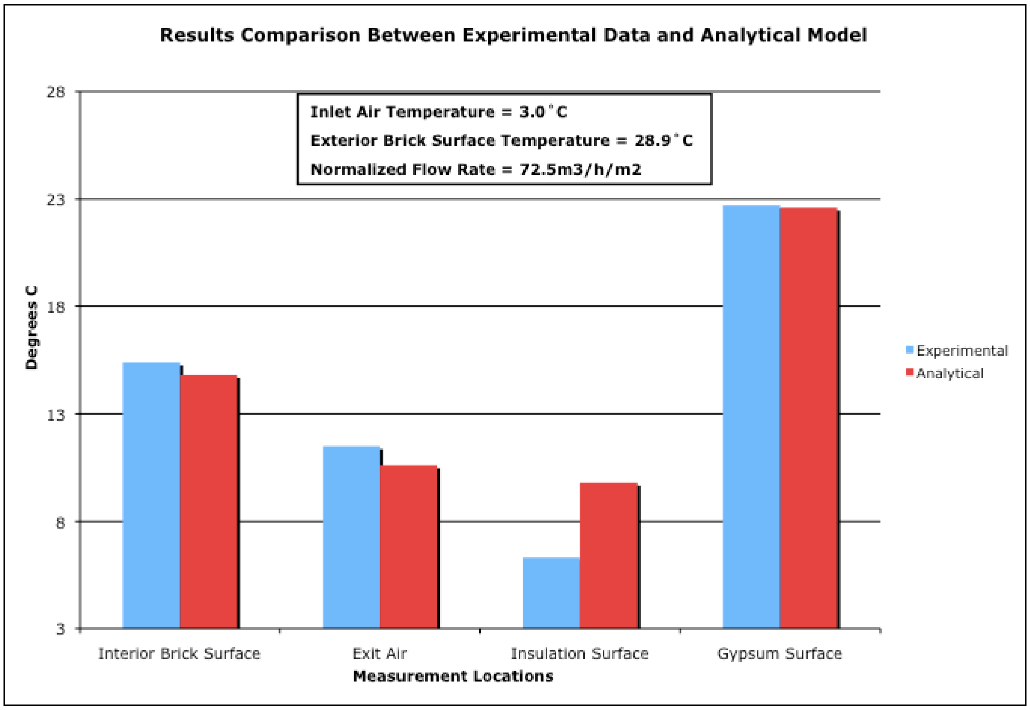

Figure 6 – Comparison of surface and air temperatures experiments and numerical model (72.5m^3/h/m^2 normalized flow rate)

The results corresponded very well, with the numerical model varying from experimental results by not more than 1˚C when predicting the temperature of the exiting air. Experimental and numerical results indicated air could be increased by as much as 13˚C at the lowest flow rate (21m^3/h/m^2). The discrepancy between the numerical model and experimental results for insulation surface temperature could be attributed to edge effects during the experiments.

Given the accuracy of the numerical model within the flow rate range of 21-72.5 m^3/h/m^2, it was then used for predicting performance criteria through simulation.

Simulating Performance

Following validation of the numerical model, assessment of performance is required. A standard method of assessing performance is the measurement of a system's effectiveness. This parameter is used in measuring the performance of commercial heat recovery ventilators and is typically calculated as shown in Equation 6. In a typical heat recovery ventilator, two streams of air cross on opposite sides of a heat exchanger and transfer heat without making contact. It is evident from this equation that an effectiveness of 1 would imply that the first air stream achieves a leaving temperature equal to the second air stream's entering temperature. This is only possible theoretically and only if the second air stream has unlimited flow.

$$e = \frac{X_2 - X_1}{X_3 - X_1} \qquad [6]$$

where,

e = effectiveness

X1 = temperature of incoming air stream before entering heat recovery ventilator

X2 = temperature of incoming air stream after leaving heat recovery ventilator

X3 = temperature of outgoing air stream before entering heat recovery ventilator

Treating the DBZ as a heat recovery ventilator requires modification of Equation 6. Rather than absorbing heat from another air stream via a heat exchanger, the DBZ wall absorbs heat from the sun and the interior via the brick and exterior insulation. Using the exterior brick temperature to replace X3, Equation 6 was modified as shown in Equation 7. Since the primary function of the DBZ in this context is to preheat ventilation air, the authors believe that Equation 7 is the most appropriate performance based comparison with heat recovery ventilators. This approach best represents the heat source from which most of the heat recovery is occurring, i.e. the Sun. Figure 7 presents the average daily effectiveness against normalized cavity flow rate for the DBZ wall.

$$e = \frac{T_{ea} - T_{ia}}{T_{eb} - T_{ia}} \qquad [7]$$

where,

e = effectiveness

Tea = DBZ exit air temperature

Tia = DBZ inlet air temperature

Teb = exterior brick temperature

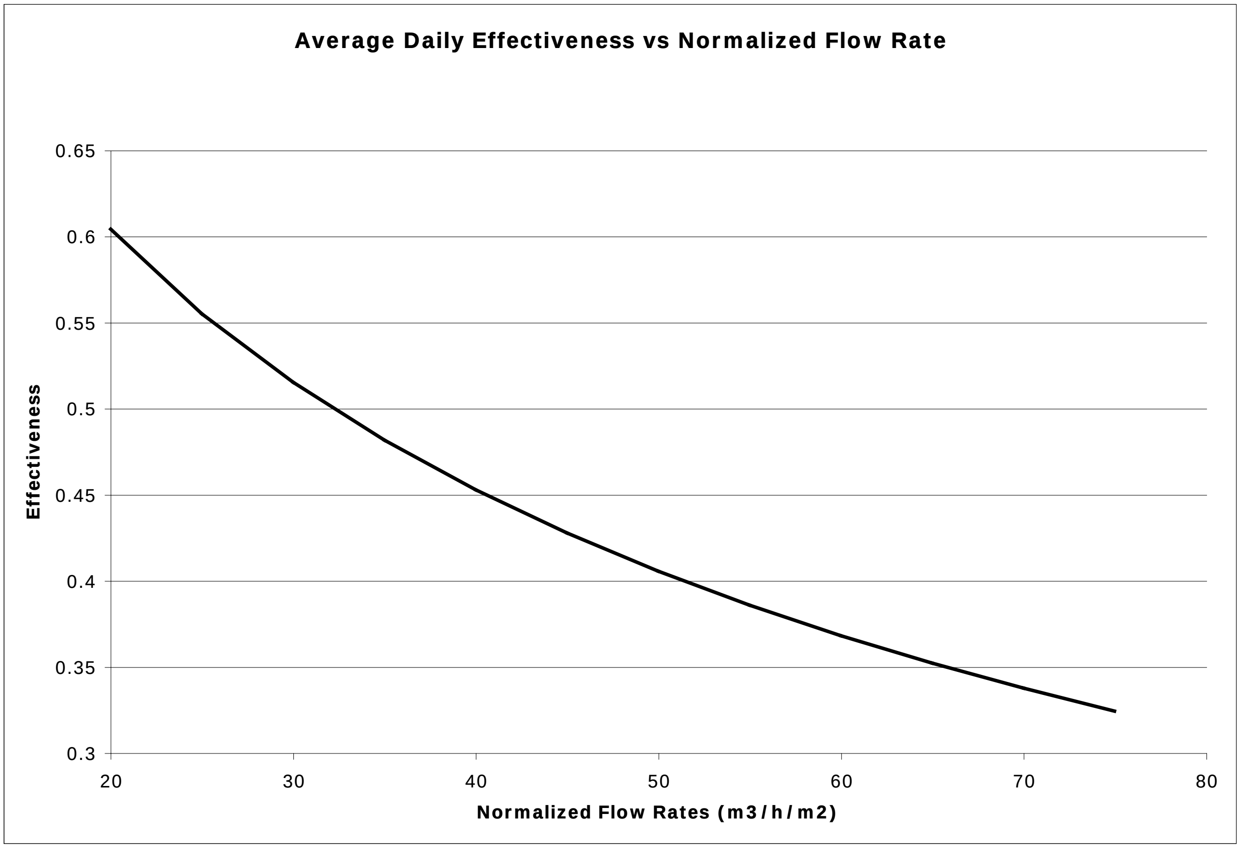

Figure 7 – Average daily effectiveness versus normalized flow rate.

In the assessment of performance criteria, two sets of data were used: (i) daily solar radiation and ambient temperature data for a sunny, January day in Toronto, Canada [28] and (ii) annual weather data for Toronto, Ontario provided by the United States Department of Energy [23].

Figure 8 shows the heat recovery distribution in watts/m^2 throughout the day for a normalized flow rate of $21m^3/h/m^2$. As expected for this system, a lag time in the heat recovered can be observed due to the high thermal storage capacity of the brick.

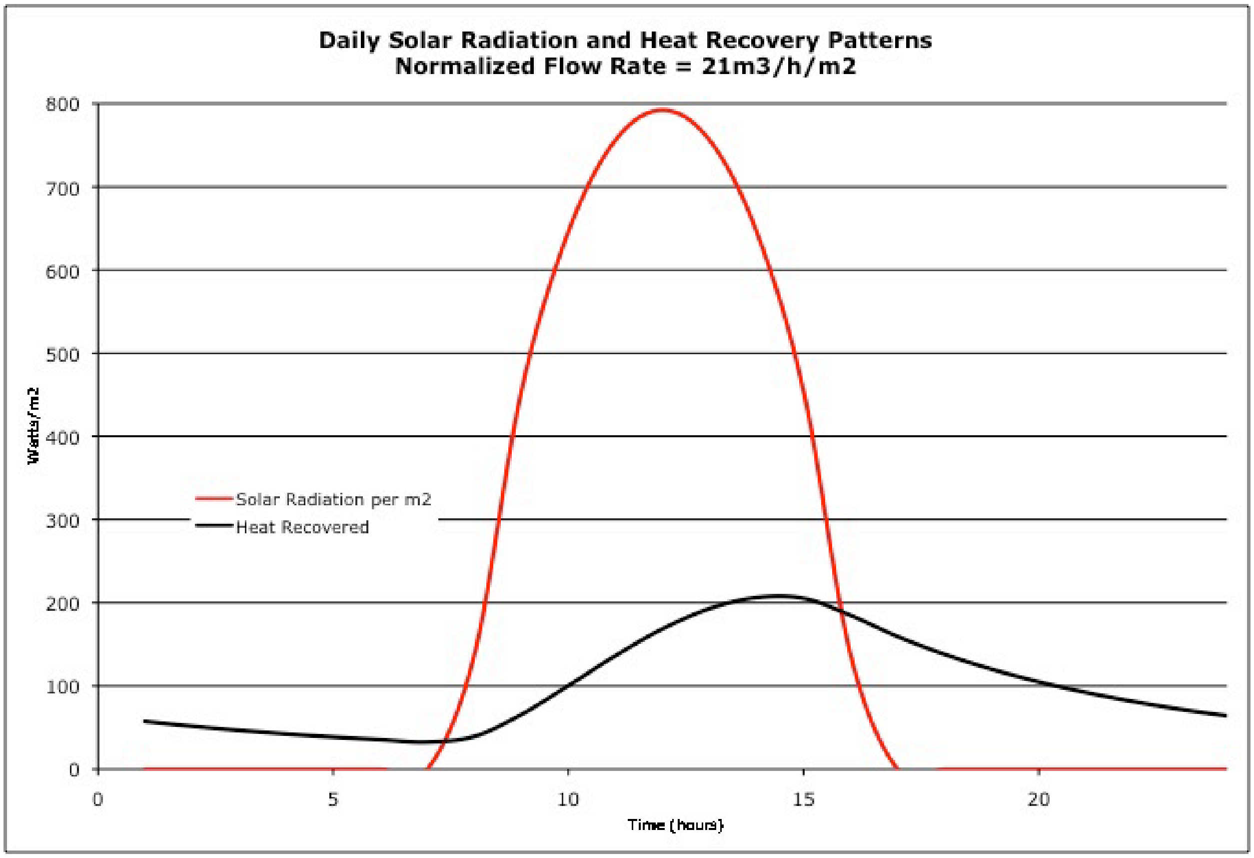

Figure 8 – Solar radiation per meter square and heat recovered daily patterns.

By defining solar efficiency as shown in Equation 8, the daily effective solar efficiency for Figure 8 was calculated to be 33%. This is admirable when compared to other solar air collecting systems with efficiencies between 20% and 40% [29].

$$\eta_{eff} = \frac{q_{HR}}{E_t A_w} \qquad [8]$$

where

η_{eff} = *effective solar efficiency*

q_{HR} = *total heat recovered (Wh)*

E_t = *solar radiation intensity* (Wh/m^2)

A_w =*wall surface area* (m^2)

Using a base $200m^2$ home, performance was simulated over an average heating season. Based on the applicable standard [30], a dwelling such as this requires $340m^3$/hour (or about 200cfm) of ventilation air. Figure 9 shows how the amount of heat recovery over a heating season changes with normalized flow rate. The range of cavity velocities used did not extend beyond the minimum and maximum amounts tested in the laboratory.

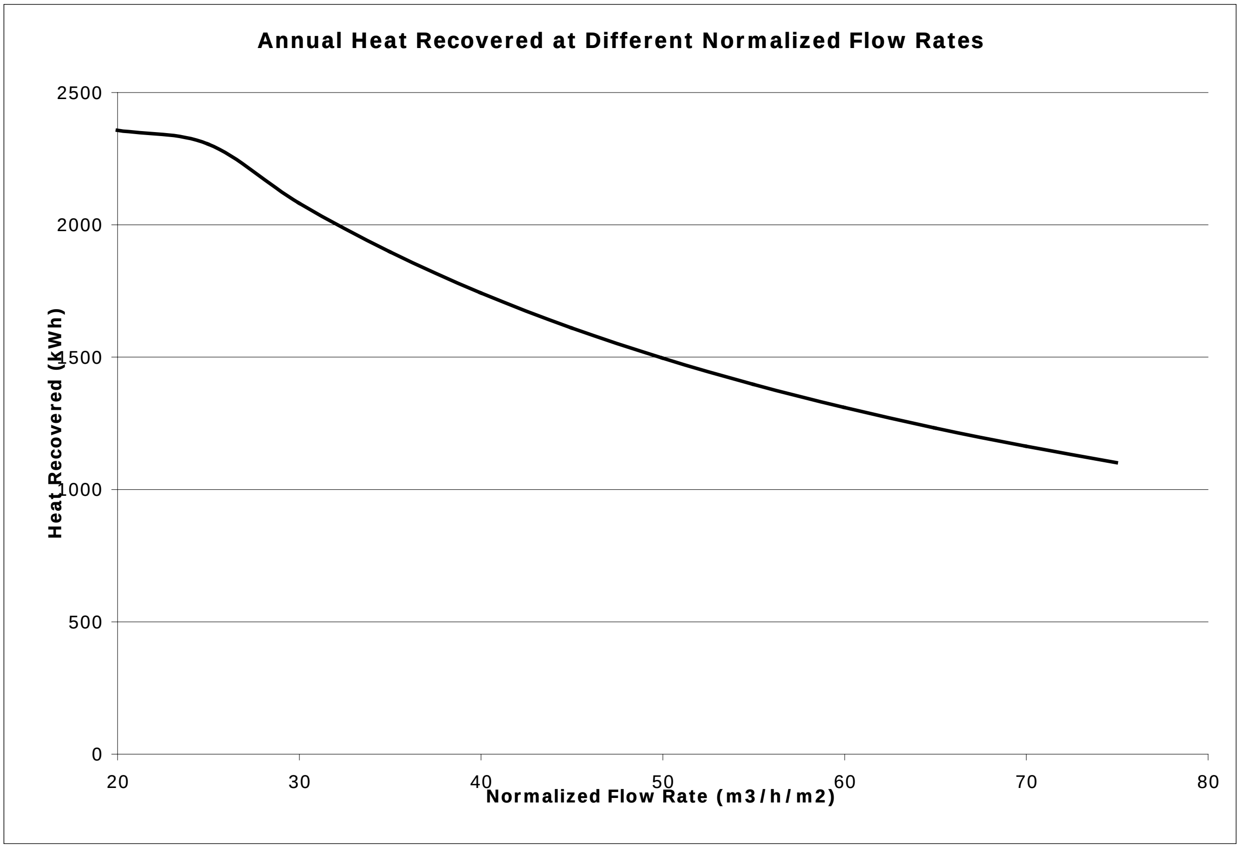

Figure 9 – Annual heat recovered at different normalized cavity flow rates.

Another common parameter for assessing performance of solar air collectors is heat recovered per collector surface area. This definition normalizes results such that useful comparisons are achieved between products. Figure 10 shows the energy savings for the DBZ wall. The savings were calculated by subtracting the required fan power from the overall collected energy. Based on the experimental regime and published values [31], a fan power required of 0.5W/m^3/h was used.

Commercial solar collector systems used to preheat ventilation air can reduce heating energy by as much as 150-210 kWh/m^2/year [24]. Although these systems are typically optimized for solar collection, they generally compromise architectural features and are used mostly in industrial applications where aesthetics is not an issue. The results in Figure 10 show the optimized DBZ wall energy savings to be approximately up to 25% the value for commercial solar air collectors used in similar applications. Given the fact that the DBZ wall is a simple modification of an existing wall assembly, these values are promising.

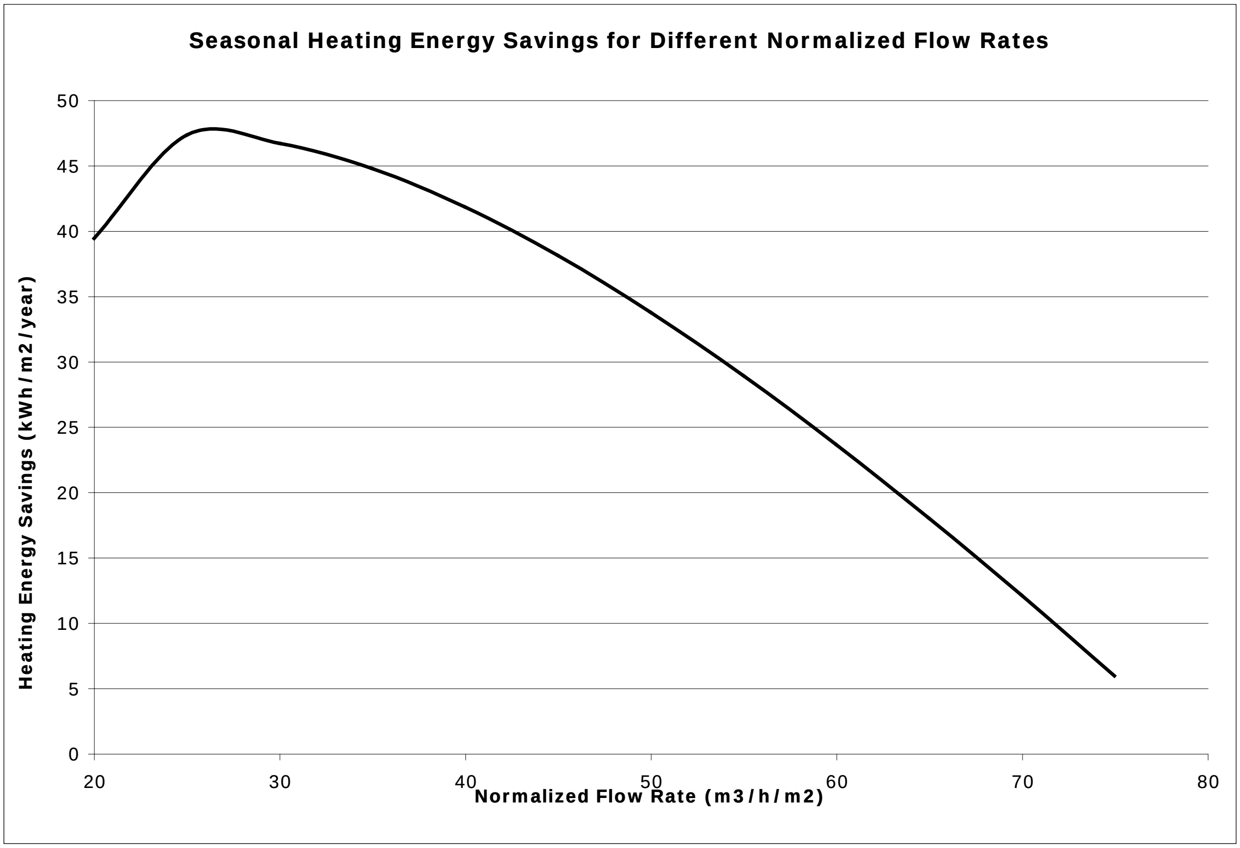

Figure 10 – Seasonal heating energy savings for different normalized flow rates.

Conclusions

The DBZ wall is an effective way of preheating ventilation air in residential applications. Using existing construction methods and practices, this approach requires little additional material, labour and operation to function. Experimental and numerical results have shown the DBZ wall could be a low cost method of saving heating energy for homes in a cold climate.

Results from the numerical model agreed well with commercial two-dimension software and full-scale model experimentation. Using the numerical model, seasonal efficiencies of 21% were predicted for flow rates providing maximum energy savings. Numerical results also indicated seasonal energy savings of up to 48 kWh/m^2 of collector surface for a standard residential dwelling. These values assume a fully exposed façade without shading from external and building elements.

Further research in the short term is required to refine the numerical model and the ability to predict performance. Long term research should focus on implantation of a full-scale DBZ wall into the construction and design of a residential dwelling. Data from such an installation can be used to improve the predictive capabilities of the numerical model.

This paper has shown through the use of existing technology and systems, traditional wall assemblies can be used to collect heating energy in an efficient manner with little or no impact on design and installation.

Acknowledgements

This research would not be completed without the financial support of the Natural Sciences and Engineering Research Council (NSERC) of Canada and it's industry partner Halcrow Yolles, Toronto, Ontario.

References

[1] NRCan, Office of Energy Efficiency. 2006. Energy Efficiency Trends in Canada: 1990 to 2004. Natural Resources Canada, Ottawa.

[2] www.homealive.ca , 2008, http://www.homealive.ca/, last accessed on May 30, 2008.

[3] healthyhousesystem.com, 2008, http://healthyhousesystem.com/toronto.html, last accessed on May 30, 2008.

[4] Morse, E. L. 1881. Warming and Ventilating Apartments by Sun's Rays. U.S. Patent 246,626.

[5] Trombe, Felix. 1972. US Patent 3,832,992.

[6] Zerrin Yilmaz, Arch Basak Kundakci, 2008, An approach for energy conscious renovation of residential buildings in Istanbul by Trombe wall system, *Building and Environment*, Volume 43, Issue 4, April, Pages 508-517.

[7] Jibao Shen, Stephane Lassue, Laurent Zalewski, Dezhong Huang, 2007, Numerical study on thermal behavior of classical or composite Trombe solar walls, *Energy and Buildings*, Volume 39, Issue 8, August, Pages 962-974.

[8] W. Smolec, A. Thomas, 1993, Theoretical and experimental investigations of heat transfer in a trombe wall, *Energy Conversion and Management*, Volume 34, Issue 5, May, Pages 385-400.

[9] R. Ben Yedder, E. Bilgen, 1991, Natural convection and conduction in Trombe wall systems, *International Journal of Heat and Mass Transfer*, Volume 34, Issues 4-5, April-May, Pages 1237-1248.

[10] S. J. Ormiston, G. D. Raithby, K. G. T. Hollands, 1986, Numerical predictions of natural convection in a trombe wall system, *International Journal of Heat and Mass Transfer*, Volume 29, Issue 6, June, Pages 869-877.

[11] Ciampi, M., F. Leccese and G. Tuoni. 2003. Ventilated Façades Energy Performance in Summer Cooling of Buildings. *Solar Energy*, 75; 491-502.

[12] Ciampi, M., F. Leccese and G. Tuoni. 2005. Energy Analysis of Ventilated and Microventilated Roofs. *Solar Energy*, 79; 183-192.

[13] Timusk, J., et al. 1992. A Systems Approach to Extend the Limit of Envelope Performance. Fifth Thermal Perforamcne of the Exterior Envelope of Buildings Conference. Clear Water, Florida.

[14] Timusk, J., 1998, The Dynamic Wall, Fourth Conference on Building Science and Technology, February 18-19, Ottawa, Canada

[15] Richman, R. and Pressnail, K., 2008, A More Sustainable Curtain Wall System: Analytical Modeling of a Solar Dynamic Buffer Zone Curtain Wall, *Building and Environment*, vol. 44, issue 1, pp. 1-10.

[16] Taylor, B., Webster, R. and Imbabi, M.S, 1999, The Building Envelope as an Air Filter, *Building and Environment*, vol. 34, pp. 353-361.

[17] Taylor, B. and Imbabi, M., 1998, The Application of DBZ Insulation in Buildings, *Renewable Energy*, vol. 15 , pp. 377-382.

[18] Salimpour-Karimi, S. 2001. Utilizing Dynamic Insulation to Improve the Performance of a Dynamic Buffer Zone, M.Eng. Project. University of Toronto, Toronto.

[19] Keller Engineering. 2003. Performance Monitoring of a Brick Veneer/Steel Stud Wall System. Canada Mortgage and Housing Corporation, Ottawa.

[20] Pasqualini, P. 1999. The Control of Moisture Movement in Buildings Using the Dynamic Buffer Zone. University of Toronto, Toronto.

[21] Pasqualini, P. 2002. The DBZ and Wall Surface Temperatures. The Canadian Architect 47, 10; 40-41.

[22] Cianfrone, C. 2007. More Sustainable Masonry Facades: Assessing the Potential to Preheat Ventilation Air Using a Solar Dynamic Buffer Zone. University of Toronto, Toronto.

[23] United States DOE. 2006. EnergyPlus Engineering Reference. United States Department of Energy, California.

[24] Eicker, U. 2003. Solar Technologies for Buildings. John Wiley & Sons, West Sussex.

[25] Berger, X., D. Buriot and F. Garnier. 1984. About the Equivalent Radiative Temperature for Clear Skies. Solar Energy 32, 6; 725-733.

[26] ASHRAE. 2001. ASHRAE Handbook: Fundamentals. American Society of Heating, Refrigeration and Air Conditioning Engineers Inc., Atlanta.

[27] Duffie, J.A. and W.A. Beckman. 1991. *Solar Engineering of Thermal Processes*, 2nd ed. John Wiley & Sons, Toronto.

[28] Hutcheon, N. and G.O.P. Handegord. 1983. Building Science For A Cold Climate. John Wiley & Sons, Toronto.

[29] Yeh, H. and Lin, T., 2005, Efficiency Improvement of Flat-Plate Solar Air Collectors, Energy, 21, 435-443.

[30] ASHRAE. 2004. ASHRAE 62-2004: Ventilation for Acceptable Indoor Air Quality. American Society of Heating, Refrigeration and Air Conditioning Engineers Inc., Atlanta.

[31] ASHRAE. 2004. ASHRAE 90.1-2004: Energy Standard For Buildings Except Low-Rise Residential Buildings. American Society of Heating, Refrigeration and Air Conditioning Engineers Inc., Atlanta.

Nomenclature

α = absorptance

A = surface area perpendicular to heat flow (m^2)

σ = Boltzmann's constant (m^2kg/s^2K)

$c_{p,b}$ = specific heat of brick (J/kg•K)

$c_{p,a}$ = specific heat of air (J/kg•K)

E_t = total surface irradiance per area (W/m^2)

$\dot{m}$ = mass flow rate (kg/s)

V_b = brick volume (m^3)

ρ_b = brick density (kg/m^3)

h_{ins} = convective coefficient between cavity air and insulation (W/m^2•K), where $Nu = 0.0158\,\mathrm{Re}^{0.8}$

h_{eb} = convective coefficient between exterior brick and environment (W/m^2•K)

$$h_{eb} = 2.537\left(\frac{PV_z}{A}\right)^{1/2} + 1.31\left(\left|T_{eb} - T_a\right|\right)^{1/3},$$

where V_z is cavity velocity

h_{ib} = convective coefficient between interior brick and cavity air (W/m^2•K)

h_{ib} = 8.29

h_i = combined radiative and convective heat transfer between interior gypsum surface and interior air (W/m^2•K)

$h_{r,grd}$ = radiative coefficient between surface and ground (W/m^2•K)

$$h_{r,gnd} = \frac{0.5\sigma\varepsilon\left(T_{eb}^4 - T_a^4\right)}{T_{eb} - T_{gnd}}$$

$h_{r,sky}$ = radiative coefficient between surface and sky (W/m^2•K)

$$h_{r,sky} = \frac{0.3535\sigma\varepsilon\left(T_{eb}^4 - T_{sky}^4\right)}{T_{eb} - T_{sky}}$$

T_a = ambient temperature (K)

T_i = interior temperature (K)

ε = emissivity

T_{ia} = cavity inlet air (K)

T_{ea} = cavity exit air (K)

$T_{f,m}$ = mean fluid temperature (K)

T_{eb} = exterior brick temperature (K)

T_{ins} = exterior insulation sheathing temperature (K)

T_{ib} = interior brick temperature (K)

T_d = ambient dew point temperature (K) T_{gyp} = interior gypsum temperature (K) T_{grd} = exterior ground temperature (K)

T_{sky} = sky temperature (K)

U_b = brick conductance

U_{ins} = effective conductance of wall assembly (includes exterior insulation, insulated stud space and gypsum board)

$h_{r,air}$ = radiative coefficient between surface and exterior air (W/m^2•K)

$$h_{r,air} = \frac{0.1465\sigma\varepsilon\left(T_{eb}^4 - T_a^4\right)}{T_{eb} - T_a}$$